THE JOURNAL OF BIOLOGICAL CHEMISTRY
Vol. 278, No. 48, Issue of November 28, pp. 48099–48104, 2003
Printed in U.S.A.

Crystal Structure of the Shank PDZ-Ligand Complex Reveals a Class I PDZ Interaction and a Novel PDZ-PDZ Dimerization*

Received for publication, June 29, 2003, and in revised form, September 2, 2003
Published, JBC Papers in Press, September 3, 2003, DOI 10.1074/jbc.M306919200

Young Jun Im‡§¶, Jun Hyuck Lee‡§, Seong Ho Park‡, Soo Jeong Park‡, Seong-Hwan Rho‡, Gil Bu Kang‡, Eunjoon Kim‖, and Soo Hyun Eom‡

From the ‡Department of Life Science, Kwangju Institute of Science and Technology, Gwangju 500-712, South Korea and ‖National Creative Research Initiative Center for Synaptogenesis, Department of Biological Sciences, Korea Advanced Institute of Science and Technology, Daejeon 305-701, Korea

The Shank/proline-rich synapse-associated protein family of multidomain proteins is known to play an important role in the organization of synaptic multiprotein complexes. For instance, the Shank PDZ domain binds to the C termini of guanylate kinase-associated proteins, which in turn interact with the guanylate kinase domain of postsynaptic density-95 scaffolding proteins. Here we describe the crystal structures of Shank1 PDZ in its peptide free form and in complex with the C-terminal hexapeptide (EAQTRL) of guanylate kinase-associated protein (GKAP1a) determined at 1.8- and 2.25-Å resolutions, respectively. The structure shows the typical class I PDZ interaction of PDZ-peptide complex with the consensus sequence -*X*-(Thr/Ser)-*X*-Leu. In addition, Asp-634 within the Shank1 PDZ domain recognizes the positively charged Arg at −1 position and hydrogen bonds, and salt bridges between Arg-607 and the side chains of the ligand at −3 and −5 positions contribute further to the recognition of the peptide ligand. Remarkably, whether free or complexed, Shank1 PDZ domains form dimers with a conserved βB/βC loop and N-terminal βA strands, suggesting a novel model of PDZ-PDZ homodimerization. This implies that antiparallel dimerization through the N-terminal βA strands could be a common configuration among PDZ dimers. Within the dimeric structure, the two-peptide binding sites are arranged so that the N termini of the bound peptide ligands are in close proximity and oriented toward the 2-fold axis of the dimer. This configuration may provide a means of facilitating dimeric organization of PDZ-target assemblies.

Multidomain Shank, proline-rich synapse-associated protein, and somatostatin receptor-interacting protein scaffold proteins bind to various membrane and cytoplasmic proteins within the PSDs[1] in excitatory synapses (1, 2). It has been suggested that Shank links *N*-methyl-D-aspartate receptor-PSD-95 complexes to the actin cytoskeleton, thereby playing a critical role in the organization of cytoskeletal signaling complexes at excitatory synapses (1, 2). The three known members of the Shank family (Shank1–3) all contain multiple sites for alternative splicing and show distinct tissue distributions (2). Although shank proteins vary in molecular mass, they share a common domain organization consisting of seven N-terminal ankyrin repeats followed by an SH3 domain, a PDZ domain, a long proline-rich region, and a SAM domain. All of these motifs are potentially involved in protein-protein interactions. For instance, the proline-rich region commonly acts as a binding site for SH3, EVH1, and WW domains and SAM domains can bind to each other in homomeric and heteromeric fashion, enabling oligomerization of Shank and its interacting proteins (3).

PDZs are globular domains containing ~80–100 amino acids (4). The Shank PDZ domain is a class I PDZ recognizing the C-terminal sequence *X*-(Thr/Ser)-*X*-Leu (where *X* represents any amino acid), which enables it to bind a variety of integral membrane proteins; however, it most specifically binds to the C terminus of GKAP, which in turn interacts with the guanylate kinase domain of PSD-95 (5). These interactions may be involved in the synaptic targeting and cytoskeletal attachment of receptors, linking them physically and functionally to the appropriate intracellular signaling pathways (5). In addition, an interaction between the Shank PDZ and the C-terminal PDZ binding motif and leucine zipper domain of βPIX was reported recently (6). βPIX is a guanidine nucleotide exchange factor that binds p21-activated kinase and promotes the functional coupling of Rac1 and Cdc42 small GTPases with downstream effector kinases (7–9).

The aim of the present study was to better understand the structural mechanism of the interaction between the Shank1 PDZ and its target protein. To that end, we determined the crystal structures of the Shank1 PDZ domain in its peptide-free form and in complex with the C-terminal hexapeptide of GKAP to resolutions of 1.8 and 2.25 Å, respectively.

EXPERIMENTAL PROCEDURES

Protein Purification and Crystallization—Recombinant Shank1 PDZ (residues 584–690) from *Rattus novergicus* with a cleavable glutathione *S*-transferase tag was expressed in *Escherichia coli* strain

* This work was supported by grant from Critical Technology 21 (Neurobiology Research Center). The costs of publication of this article were defrayed in part by the payment of page charges. This article must therefore be hereby marked "*advertisement*" in accordance with 18 U.S.C. Section 1734 solely to indicate this fact.

The atomic coordinates and structure factors (codes 1Q3O and 1Q3P) have been deposited in the Protein Data Bank, Research Collaboratory for Structural Bioinformatics, Rutgers University, New Brunswick, NJ (http://www.rcsb.org/).

§ Both authors contributed equally to this work.

¶ Supported by Brain Korea 21 and Kwangju Institute of Science and Technology projects.

** To whom correspondence should be addressed: Dept. of Life Science, Kwangju Institute of Science and Technology, Gwangju 500-712, South Korea. Tel.: 82-62-970-2549; Fax: 82-62-970-2548; E-mail: eom@kjist.ac.kr.

[1] The abbreviations used are: PSD, postsynaptic density; PDZ, PSD/discs large/ZO-1; GKAP, guanylate kinase-associated protein; SH3, Src homology 3; SAM, sterile α-motif; EVH1, Ena/VSAP homology 1; MAD, multiple anomalous dispersion; GRIP, glutamate receptor-interacting protein; NHERF, Na^+/H^+ exchanger regulatory factor; r.m.s., root mean square.

TABLE I
Data collection and refinement statistics

Data set	Peptide-free (Br-MAD)[a]			PDZ-peptide complex
Crystal form	$P2_1$			$P4_12_12$
X-ray source	BL-18B (Photon Factory)			6B (PAL)
Wavelength	λ1	λ2	λ3	1.000
	0.9202	0.9192	0.900	
Resolution (Å)	27.7-1.8			30–2.25
R_{sym}[b] (%)	4.8 (37.7)	4.8 (32.6)	4.9 (33.7)	4.1 (25.8)
Data coverage total/final shell (%)	99.0 (99.0)	99.0 (99.0)	99.0 (99.0)	96.2 (95.6)
Phasing (34.5-1.9 Å)	0.52 (RESOLVE)			
Overall figure of merit				
Refinement				
R_{cryst}[c] total (%)	23.4			25.1
R_{free}[d] total (%)	25.1			28.0
R.m.s. bond length (Å)	0.006			0.007
R.m.s. bond angle (°)	1.2			1.3
Average B-value (Å^2)	32.2			43.7

[a] Derivatized by crystallizing the protein in solution containing 200 mM NaBr.
[b] $R_{sym} = \langle I \rangle - I\langle I \rangle$.
[c] $R_{cryst} = \langle |F_o| - |F_c| \rangle / |F_o|$.
[d] R_{free} calculated using 5% of all reflections excluded from the refinement stages.

BL21(DE3) and then purified and crystallized as described previously (10). The C-terminal hexapeptide (EAQTRL) of GKAP used for PDZ-peptide cocrystallization was chemically synthesized (Anygen).

Data Collection—A MAD data set was collected from a peptide-free frozen crystal to a resolution of 1.8 Å using an ADSC Quantum 4R CCD detector at beamline 18B at the Photon Factory. Because bromine is a convenient anomalous scatterer for MAD phasing, a bromine MAD data set was collected from a single crystal crystallized in a solution containing 200 mM NaBr (11). The diffraction data from a PDZ-peptide complex to a resolution of 2.25 Å were collected at 100 K at beamline 6B of the Pohang Accelerator Laboratory.

Structure Determination and Refinement—The structure of the peptide-free PDZ domain was determined by MAD phasing using bromine as an anomalous scatterer. The positions of three bromines within the asymmetric unit were located and refined using the program SOLVE (12). The initial phases were improved by solvent flattening using the program RESOLVE (overall figure of merit, 0.52) (13). The resultant map, showing a dimer in an asymmetric unit, was readily interpretable. Model building then proceeded using the program O (14), after which the structure was refined using the program CNS (15). The final crystallographic R value for the peptide-free PDZ model, calculated using data from 27.7–1.8 Å, was 23.4% (R_{free} = 25.1%).

Using the structure of the peptide-free PDZ dimer served as a starting model, the structure of the PDZ-hexapeptide complex was determined by molecular replacement methods with the program MOLREP (16). There were two PDZ domains related by non-crystallographic 2-fold symmetry within the asymmetric unit. After applying a simulated annealing procedure using data to 2.25 Å, the locations of the two bound peptides were determined from a $F_o - F_c$ difference electron density map. The electron densities for all of the six residues of the peptide ligands were obvious, indicating that they were well ordered within the structure. The hexapeptide was modeled using program O, after which the ligand-bound PDZ domain was refined to a final crystallographic R value of 25.1% and a free R value of 28.0%. The refined model of the peptide-bound PDZ domain consisted of a PDZ dimer related by a non-crystallographic 2-fold axis, two hexapeptides, and 44 water molecules. The stereochemistry of the model was analyzed with PROCHECK (17). No residues were found in the disallowed regions of the Ramachandran plot. Data collection and refinement statistics are summarized in Table I.

RESULTS AND DISCUSSION

Overall Structure of the Shank1 PDZ Domain—The Shank1 PDZ monomer is a compact, globular domain containing eight segments of secondary structure: six β strands that form an antiparallel β barrel and two α helices (Fig. 1*A*). The amino acid sequences of all of the Shank protein PDZ domains are nearly identical but differ significantly from other PDZ domains (Fig. 1*B*) (18, 19). The amino acid sequence of the rat Shank1 PDZ domain (residues 582–690) used in this study is identical to the human domain and shares 88 and 77% sequence identity with the PDZ domains of rat Shank2 and Shank3, respectively. The overall fold of the Shank1 PDZ shows the highest degree of structural variation of any known PDZ (Fig. 1*C*). In addition, the Shank1 PDZ contains exceptionally long N-terminal βA and C-terminal βF strands, which span more >11 residues each and participate in antiparallel β sheet interactions. The βA strand is twisted and participates in dimeric interaction by forming an antiparallel β sheet with the βA strand of the other monomer (Fig. 1*C*). The PDZ domain segment that displays the most conformational variation is the loop connecting the βB and βC strands. The Shank1 PDZ contains the longest known βB/βC loop, spanning 19 residues. Despite the variability in the sequence and length of βB/βC loops, the sequence is strictly conserved among Shank PDZ domains.

As is typical of most PDZ complexes, the peptide ligand is positioned within a groove between the βB strand and the αB helix, oriented as an additional strand antiparallel to βB. Within the crystal structure of the complex, all six amino acid residues of the peptide ligand were well defined as shown by the difference electron density map calculated without inclusion of the peptide. Superposition of the structures of the peptide-free and peptide-bound PDZ domain shows that there is little conformational change upon ligand binding. The C_α root mean square (r.m.s.) deviation between two models is only 0.69 Å.

Structural Basis for the Specificity of the Shank1 PDZ-GKAP Interaction—PDZ domains typically bind to the last several residues at the C terminus of interacting proteins. Shank PDZ domains are known to bind to the C-terminal six residues of GKAP1a, which in turn associates with the guanylate kinase domain of PSD-95 (20). Although they recognize the typical consensus sequence *X*-(Thr/Ser)-*X*-Leu and are classified as type I PDZ domains, Shank PDZ domains show higher specificity for the GKAP C-terminal EAQTRL sequence. The interaction with GKAP is reportedly specific for the Shank PDZ, because GKAP1a (residues 591–666) does not associate with the other class I PDZ domains (*e.g.* those of PSD-95, Chapsyn-110/PSD-93, or calmodulin-dependent serine kinase) (3). Moreover, the C-terminal tail of Kv1.4 (ETDV) does not bind the Shank PDZ, even though it interacts with the PDZ domains of PSD-95 (3). The Shank PDZ domain is thus optimized for recognition of GKAP, even though it marginally binds other ligands via the consensus sequence.

Within the crystal structure, the peptide ligand EAQTRL inserts into the binding pocket antiparallel to the βB strand, forming an extensive network of hydrogen bonds and hydro-

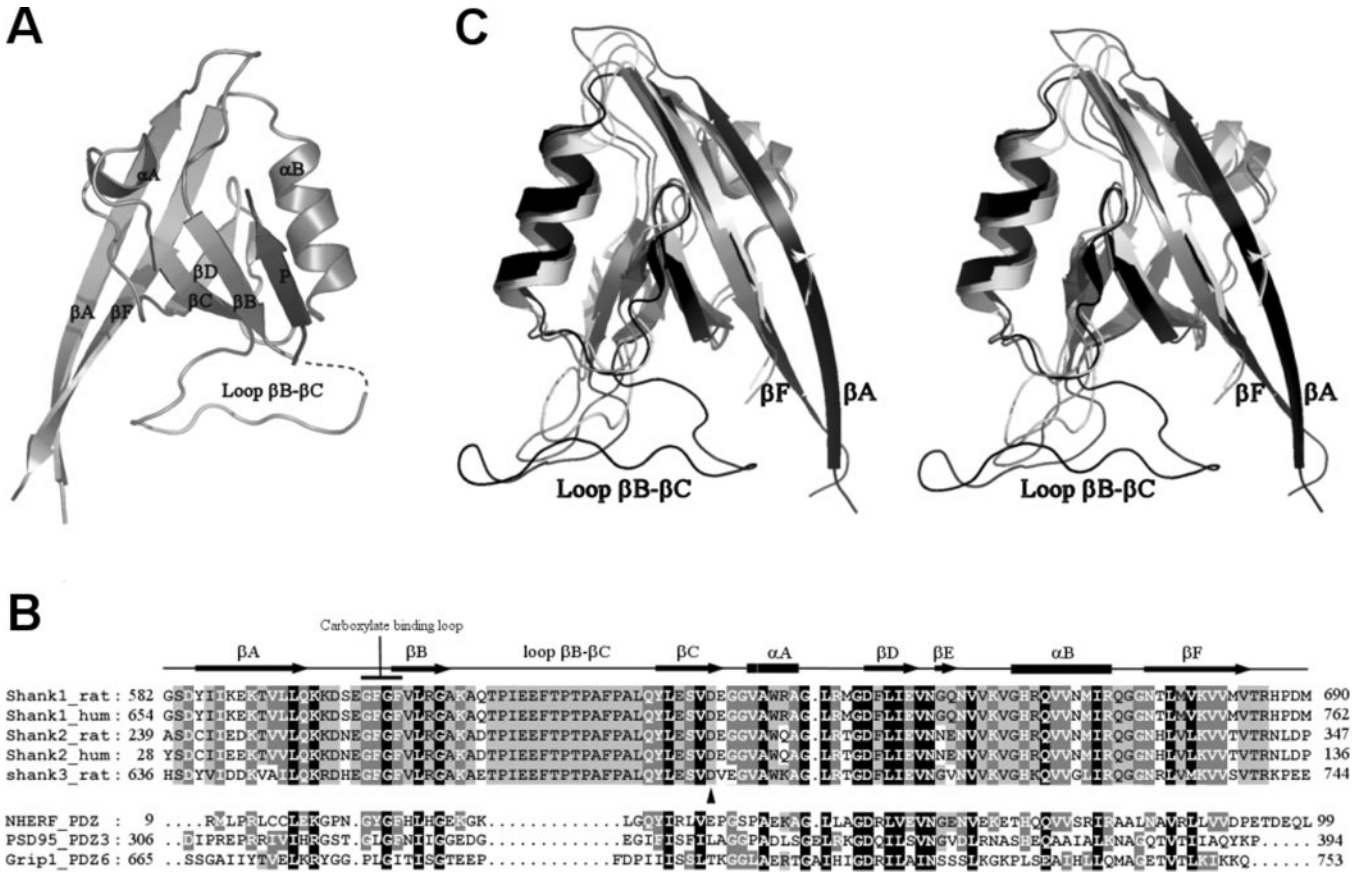

FIG. 1. **Structure of the SHANK1 PDZ domain.** *A*, stereoview of a ribbon diagram showing the monomeric structure of the Shank PDZ-ligand complex. The β-strands are labeled βA–βF, and the α-helices are labeled αA and αB. The ligand is colored *dark gray*. The *dotted line* indicates a disordered loop (residues 610–614) that is not seen in peptide-bound structure. All of the residues in the loop were observed in peptide-free structure. *B*, amino acid sequence alignment of the PDZ domains from the rat and human Shank family, human NHERF (37), rat PSD95 (26), and rat GRIP1 (35). The sequences were aligned using the program ClustalX (38). Highly conserved residues are shaded in *black* and *gray*. The secondary structure elements of Shank1 PDZ are shown as *arrows* (β-strands), *bars* (α-helices), and *lines* (connecting loops). *C*, superposition of the PDZ domains. *Black ribbon* indicates Shank1 PDZ domain. *Light* and *dark gray ribbons* indicate PDZ domains of human NHERF (Protein Data Bank code 1G9O) and rat PSD95 (Protein Data Bank code 1BFE), respectively.

phobic interactions (Fig. 2, *A* and *B*). The GFGF sequence in the carboxylate binding loop of the Shank1 PDZ forms hydrogen bonds with the carboxyl group of the GKAP peptide C terminus in a manner similar to that seen previously in PDZ-ligand complexes. The backbone amides of Phe-602, Gly-603, and Phe-604 of the carboxylate binding loop are involved in hydrogen bonding with the C terminus of the ligand, whereas the side chain of Leu-0 enters the deep hydrophobic cavity formed by Phe-602, Phe-604, Leu-606, and Ile-670.

Instead of the side chain of the penultimate residue of the ligand being oriented toward the solvent, the Shank1 PDZ interacts directly with the −1 position of the ligand (Fig. 2*B*). The carboxyl group of Asp^{634} located at the end of the βC strand forms a salt bridge with the guanido group of Arg^{-1}. To do so, the long side chain of Arg^{-1} twists at the Cβ atom toward Asp^{634}. Sequence alignment shows that Asp^{634} is strictly conserved among all of the Shank proteins characterized so far (rat Shank1–3 and human Shank1 and Shank2). Moreover, all of the known GKAP family proteins (GKAP/SAP90/PSD-95-associated protein 1–4) terminate with the same four amino acids (−QTRL) (21). This finding suggests that a positively charged residue is greatly preferred at ligand position −1 because it directly contributes to the specificity of the PDZ-ligand interaction. Consistent with that idea, substituting Arg^{-1} with Glu significantly reduced the affinity of the interaction (3). The preference for a positively charged residue at the −1 position was previously reported in the NHERF PDZ1-cystic fibrosis transmembrane conductance interaction where Glu^{43} serves a function equivalent to that of Asp^{634} in the Shank PDZ (22). In addition, Erbin PDZ domain selectively accommodates ligands with a bulky hydrophobic side chain of tryptophan residue at the −1 position, revealing the contribution of penultimate residues to the optimal binding of the ligands (23).

In class I PDZ domains, serine or threonine at the −2 position of the ligand forms a hydrogen bond with the side chain of residues at the start of helix αB. Likewise, within the Shank PDZ-ligand complex, the threonine residue at ligand position −2 contributes to the specificity by hydrogen bonding with His^{663} at αB1 (Fig. 2*B*).

The ligand residues at the −3 and −5 positions also appear to contribute to the specificity and affinity of the interaction. Involvement of the residues at the −3 position in the PDZ-ligand interaction was reported in diverse types of PDZ domains (22–26). In Shank PDZ domain, the guanido group of Arg^{607} in the βB strand is positioned within the groove formed by the protrusions of the side chains of Gln^{-3} and Glu^{-5}. The Oε atom of Gln^{-3} forms hydrogen bonds with the Arg^{607}guanido group, and Glu^{-5} interacts both with the side chain of Arg^{607} and the hydroxyl group of Tyr^{629}. This means that the presence of Arg^{607} may further stabilize the interaction by hydrogen bonding with the hydrophilic residues at positions −3 and −5, even though interactions at those positions are not essential for ligand binding.

Dimerization of PDZ Domains—Several well characterized PSD scaffold proteins, including PSD-95 (27, 28), the Homer family of proteins (29), and GRIP/AMPA receptor-binding pro-

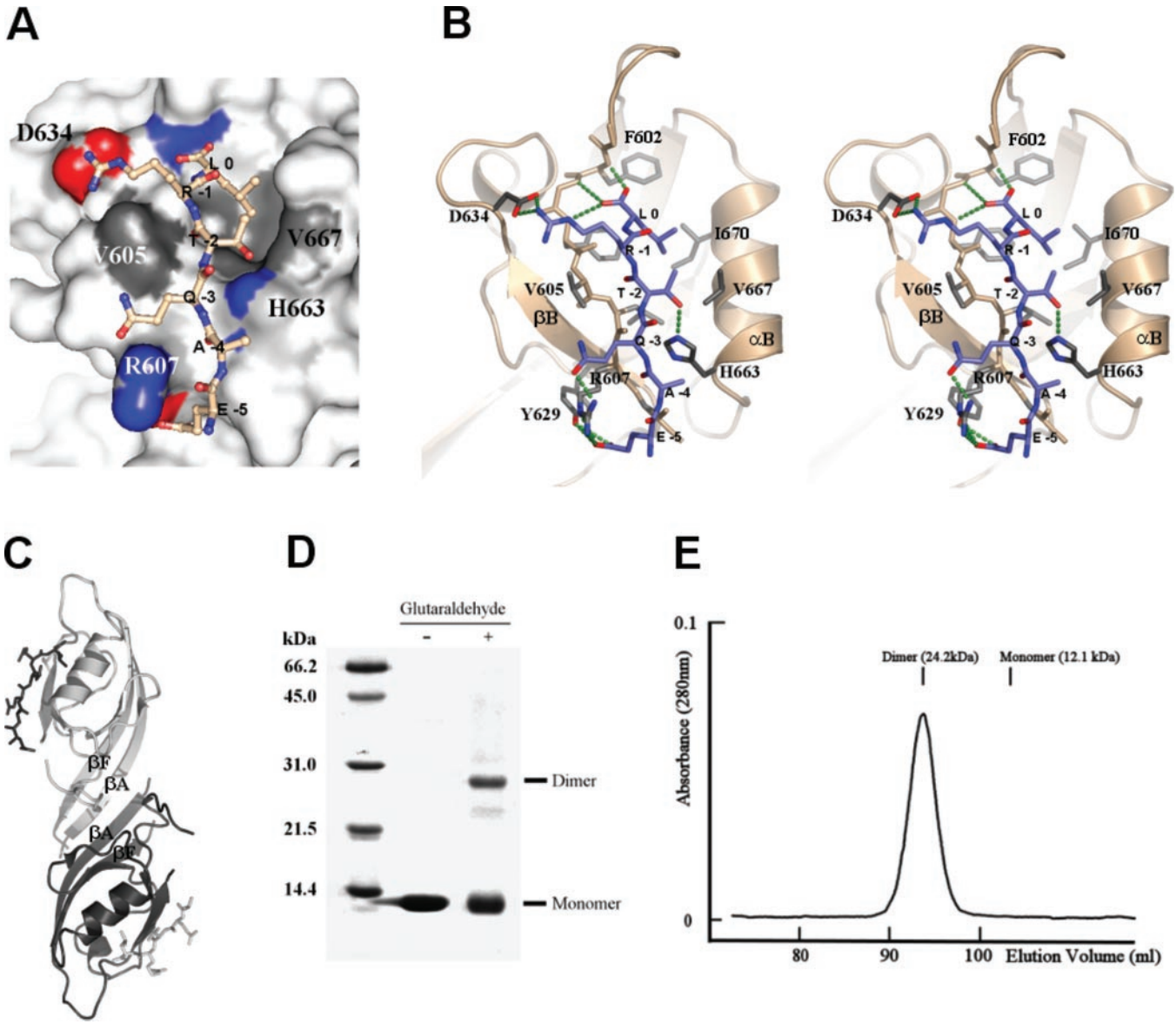

FIG. 2. *A*, molecular surface of the peptide binding pocket in the Shank1 PDZ domain. The bound peptide is shown as a *ball* and *stick model*. The hydrophobic residues in the binding pocket are colored in *dark gray*. The acidic and basic residues are *colored red* and *blue*, respectively. *B*, stereoview of a *ball* and *stick model* of the peptide binding pocket and its specific ligand (EAQTRL). *Dashed lines* represent hydrogen bonds or salt bridges between the ligand and the PDZ domain. *C*, dimeric structure of the Shank1 PDZ domain. Peptide ligands were shown as ball and stick models. *D*, SDS-PAGE showing the result of chemical cross-linking of purified Shank1 PDZ domain incubated with 0.1% glutaraldehyde for 10 min. *E*, Superdex 200 (Amersham Biosciences) gel filtration profile of the native Shank1 PDZ domain shows the existence of Shank1 PDZ dimers in solution. The two experiments summarized in *panels D* and *E* both indicate a dimeric form for the Shank PDZ domain in solution.

tein (30), have the ability to form homomultimers or heteromultimers. And in some cases, such multimerization is mediated by the PDZ domains (31–33). For example, this was recently seen in the crystal structure of GRIP PDZ6, which shows a tightly associated dimer (34). In Shank proteins, the SAM domain reportedly multimerizes, which is sufficient for self-association of full-length Shank proteins; however, the present study shows that the PDZ domain also contributes to the multimerization of Shank proteins, suggesting structural conservation of a dimerization mode mediated by PDZ domains.

The crystal structures revealed tightly associated dimers in the asymmetric units of both the peptide free and peptide bound crystals, which belong to the $P2_1$ and $P4_12_12$ space groups, respectively (Fig. 2*C*). Each asymmetric unit contained two molecules forming a dimer with non-crystallographic 2-fold symmetry. Cross-linking experiments and size-exclusion chromatography confirmed the Shank1 PDZ to be a dimer in solution (Fig. 2, *D* and *E*). That the Shank1 PDZ domain has the ability to form a dimer whether it is free or complexed with a ligand suggests the dimer may represent the functional state of the Shank PDZ domain.

The interface between dimeric PDZ domains involves a βA strand and a βB/βC loop from each monomer (Fig. 3, *A* and *C*). The βA strands form antiparallel β-sheets around the center of a 2-fold axis so that the N and C termini of each PDZ domain point in opposite directions. The amount of surface area buried upon dimer formation is 611.6 $Å^2$ or 9.5% of the total surface area of each monomer, which implies the existence of specific contacts between the two monomers that may have biological significance. The dimeric interface is composed of 64.9% of non-polar atoms and 35.0% of polar atoms. Within the dimer, the monomers are held tightly by six hydrogen bonds, four water-bridged hydrogen bonds, and numerous van der Waals interactions. All of the six hydrogen bonds originate from backbone atoms in the βA strands forming the antiparallel β-sheet.

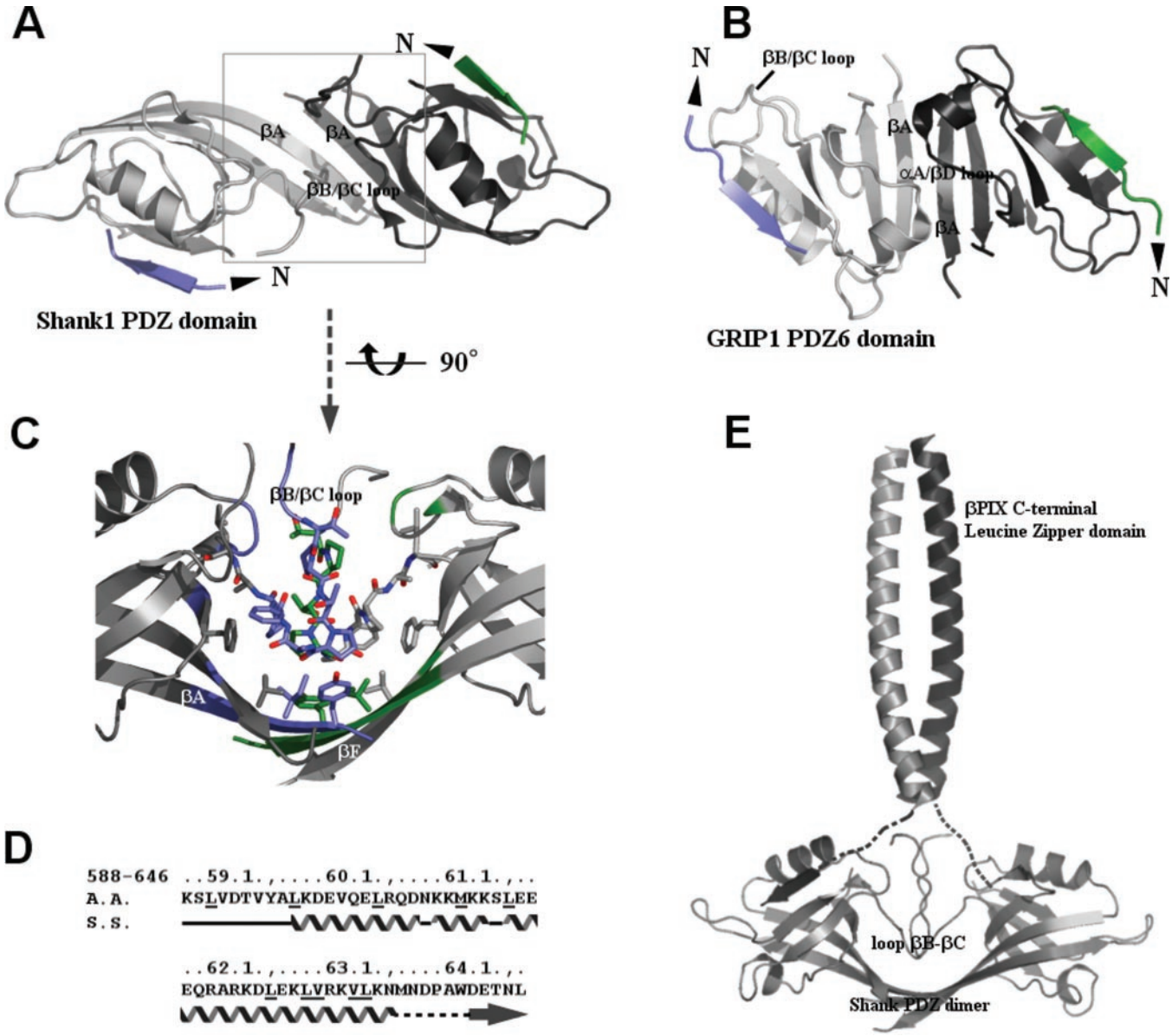

FIG. 3. **Overall structures of the PDZ dimer.** *A*, Shank1 PDZ dimer. The *black arrow* indicates the N-terminal end of each peptide ligand. *B*, ribbon diagram of the GRIP PDZ6 dimer (Protein Data Bank code 1N7F). *C*, Shank PDZ dimer interface. Side chains of hydrophobic residues at the interface are shown as *ball* and *stick models*. *D*, amino acid sequence and predicted secondary structure of the C-terminal domain of βPIX. The secondary structure was predicted using the PredictProtein Web server (cubic.bioc.columbia.edu/predictprotein/). *E*, proposed model of the Shank1 PDZ and βPIX C terminus complex. The figures were made using PyMOL (www.pymol.org).

In contrast, mostly side chain atoms in the βB/βC loops, which comprises 41% of the interface area, participate in the hydrophobic interactions at the interface. That residues 613–625 in the otherwise variable βB-βC loop are strictly conserved in all of the Shank proteins identified so far implies a potential role for the βB/βC loop in both dimerization and protein-protein interactions. Recently, the crystal structure of Erbin PDZ·ErbB2 complex revealed the important function of the loop βB-βC in ligand interactions, implying the possibility that the variable loop βB-βC could be exploited for the specific function of the PDZ domain (24).

Similar to Shank PDZ, GRIP PDZ6 dimerizes by forming antiparallel β-sheets with N-terminal βA strands (Fig. 3, *A* and *B*), although the configurations of the βA strands differ in the two dimers (34). Shank PDZ has a longer more twisted βA strand, and half of the strand is involved in the β-sheet interaction causing the peptide binding pockets to be oriented differently. In both dimers, the peptide binding pockets are located at the distal sides of the complex and oriented in antiparallel fashion. In the Shank PDZ dimer, however, the N termini of the ligands are oriented toward the center so that they are in close proximity around the 2-fold axis of the dimer (Fig. 3*A*).

Biological Implications of Shank PDZ Dimer—Shank proteins have a SAM domain at their C terminus, which can mediate oligomerization of the proteins. Sharpin, which interacts with Shank anykrin repeats, has a coiled-coil domain that contributes to the multimeric association of the Shank-Sharpin complex (35). Notably, the crystal structure of the Shank1 PDZ domain suggests that the dimeric configuration of the PDZ domain may facilitate multimeric organization of Shank proteins. Although multimeric association of GKAP and Shank PDZ has yet to be reported, the interaction of βPIX and Shank PDZ provides some insight to the biological significance of the Shank PDZ dimer. The Shank1 PDZ domain reportedly interacts with the C-terminal domain of βPIX, and the leucine zipper domain mediates the homodimerization of βPIX (6, 36). This means that both the C-terminal PDZ binding motif and the preceding leucine zipper domain of βPIX are involved in the

interaction and that an additional interaction besides that taking place at the peptide binding pocket of the PDZ domain is involved in the binding of βPIX (6). The leucine zipper motif commonly forms a coiled-coil homodimer of two α-helices terminating at their C termini with a 2-fold symmetry. Prediction of βPIX secondary structure indicates that six amino acid residues connect the C-terminal PDZ binding motif and the preceding leucine zipper helix (Fig. 3*D*). As mentioned above, the ligands binding to the PDZ are in close proximity around the 2-fold axis of the dimer. And given the strict conservation of the βB/βC loop among Shank proteins, there are few tertiary configurations available to the PDZ-βPIX complex. With that in mind, we propose a model of the Shank PDZ-βPIX C-terminal complex in which the C-terminal root of the leucine zipper domain interacts with the βB-βC loops at the center of PDZ dimer and the C-terminal tails are inserted into the peptide binding pockets (Fig. 3*E*). This model suggests that the novel surface interacting with the leucine zipper domain is the conserved βB/βC loop. Such a configuration is advantageous, because it would enable dimeric PDZ domains to efficiently colocalize with dimeric target proteins.

Acknowledgments—We thank Professor N. Sakabe and Drs. M. Suzuki and N. Igarashi for their kind support with x-ray data collection at beamline BL-18B of Photon Factory (Tsukuba, Japan). We also thank Dr. H. S. Lee and G. H. Kim at the BL6B of Pohang Accelerator Laboratory (Pohang, Korea).

REFERENCES

1. Sheng, M., and Kim, E. (2000) *J. Cell Sci.* **113,** 1851–1856
2. Boeckers, T. M., Bockmann, J., Kreutz, M. R., and Gundelfinger, E. D. (2002) *J. Neurochem.* **81,** 903–910
3. Naisbitt. S., Kim, E., Tu, J. C., Xiao, B., Sala, C., Valtschanoff, J., Weinberg, R. J., Worley, P. F., and Sheng, M. (1999) *Neuron* **23,** 569–582
4. Sheng, M., and Sala, C. (2001) *Annu. Rev. Neurosci.* **24,** 1–29
5. Yao, I., Hata, Y., Hirao, K., Deguchi, M., Ide, N., Takeuchi, M., and Takai, Y. (1999) *J. Biol. Chem.* **274,** 27463–27466
6. Park, E., Na, M., Choi, J., Kim, S., Lee, J. R., Yoon, J., Park, D., Sheng, M., and Kim, E. (2003) *J. Biol. Chem.* **278,** 19220–19229
7. Manser, E., Loo, T. H., Koh, C. G., Zhao, Z. S., Chen, X. Q., Tan, L., Tan, I., Leung, T., and Lim, L. (1998) *Mol. Cell* **1,** 183–192
8. Bagrodia, S., Taylor, S. J., Jordon, K. A., Van Aelst, L., and Cerione, R. A. (1998) *J. Biol. Chem.* **273,** 23633–23636
9. Oh, W. K., Yoo, J. C., Jo, D., Song, Y. H., Kim, M. G., and Park, D. (1997) *Biochem. Biophys. Res. Commun.* **235,** 794–798
10. Park, S. H., Im, Y. J., Rho, S. H., Lee, J. H., Yang, S., Kim, E., and Eom, S. H. (2002) *Acta Crystallogr. Sect. D Biol. Crystallogr.* **58,** 1353–1355
11. Dauter, Z., Dauter, M., and Rajashankar, K. R. (2000) *Acta Crystallogr. Sect. D Biol. Crystallogr.* **56,** 232–237
12. Terwilliger, T. C., and Berendzen, J. (1999) *Acta Crystallogr. Sect. D Biol. Crystallogr.* **55,** 849–861
13. Terwilliger, T. C., and Berendzen, J. (1999) *Acta Crystallogr. Sect. D Biol. Crystallogr.* **55,** 1863–1871
14. Jones, T. A., Zou, J.-Y., Cowan, S. W., and Kjeldgaard, M. (1991) *Acta Crystallogr. Sect. A* **47,** 110–119
15. Brunger, A. T., Adams, P. D., Clore, G. M., DeLano, W. L., Gros, P., Grosse-Kunstleve, R. W., Jiang, J.-S., Kuszewski, J., Nilges, N., Pannu, N. S., Read, R. J., Rice, L. M., Simonson, T., and Warren, G. L. (1998) *Acta Crystallogr. Sect. D Biol. Crystallogr.* **54,** 905–921
16. Vagin, A., and Teplyakov, A. (1997) *J. Appl. Crystallogr.* **30,** 1022–1025
17. Laskowski, R. A., MacArthur, M. W., Moss, D. S., and Thornton, J. M. (1993) *J. Appl. Crystallogr.* **26,** 283–291
18. Boeckers, T. M., Kreutz, M. R., Winter, C., Zuschratter, W., Smalla, K. H., Sanmarti-Vila, L., Wex, H., Langnaese, K., Bockmann, J., Garner, C. C., and Gundelfinger, E. D. (1999) *J. Neurosci.* **19,** 6506–6518
19. Lim, S., Naisbitt, S., Yoon, J., Hwang, J. I., Suh, P. G., Sheng, M., and Kim, E. (1999) *J. Biol. Chem.* **274,** 29510–29518
20. Kim, E., Naisbitt, S., Hsueh, Y. P., Rao, A., Rothschild, A., Craig, A. M., and Sheng, M. (1997) *J. Cell Biol.* **136,** 669–678
21. Takeuchi, M., Hata, Y., Hirao, K., Toyoda, A., Irie, M., and Takai, Y. (1997) *J. Biol. Chem.* **272,** 11943–11951
22. Karthikeyan, S., Leung, T., and Ladias, J. A. (2001) *J. Biol. Chem.* **276,** 19683–19686
23. Laura, R. P., Witt, A. S., Held, H. A., Gerstner, R., Deshayes, K., Koehler, M. F., Kosik, K. S., Sidhu, S. S., and Lasky, L. A. (2002) *J. Biol. Chem.* **277,** 12906–12914
24. Birrane, G., Chung, J., and Ladias, J. A. (2003) *J. Biol. Chem.* **278,** 1399–1402
25. Kimple, M. E., Siderovski, D. P., and Sondek, J. (2001) *EMBO J.* **20,** 4414–4422
26. Doyle, D. A., Lee, A., Lewis, J., Kim, E., Sheng, M., and MacKinnon, R. (1996) *Cell* **85,** 1067–1076
27. Kim, E., Cho, K. O., Rothschild, A., and Sheng, M. (1996) *Neuron* **17,** 103–113
28. Hsueh, Y. P., Kim, E., and Sheng, M. (1997) *Neuron* **18,** 803–814
29. Xiao, B., Tu, J. C., Petralia, R. S., Yuan, J. P., Doan, A., Breder, C. D., Ruggiero, A., Lanahan, A. A., Wenthold, R. J., and Worley, P. F. (1998) *Neuron* **21,** 707–716
30. Srivastava, S., Osten, P., Vilim, F. S., Khatri, L., Inman, G., States, B., Daly, C., DeSouza, S., Abagyan, R., Valtschanoff, J. G., Weinberg, R. J., and Ziff, E. B. (1998) *Neuron* **21,** 581–591
31. Xu, X. Z., Choudhury, A., Li, X., and Montell, C. (1998) *J. Cell Biol.* **142,** 545–555
32. Lau, A. G., and Hall, R. A. (2001) *Biochemistry* **40,** 8572–8580
33. Dong, H., Zhang, P., Song, I., Petralia, R. S., Liao, D., and Huganir, R. L. (1999) *J. Neurosci.* **19,** 6930–6941
34. Im, Y. J., Park, S. H., Rho, S. H., Lee, J. H., Kang, G. B., Sheng, M., Kim, E., and Eom, S. H. (2003) *J. Biol. Chem.* **278,** 8501–8507
35. Lim, S., Sala, C., Yoon, J., Park, S., Kuroda, S., Sheng, M., and Kim, E. (2001) *Mol. Cell Neurosci.* **17,** 385–397
36. Kim, S., Lee, S. H., and Park, D. (2001) *J. Biol. Chem.* **276,** 10581–10584
37. Karthikeyan, S., Leung, T., Birrane, G., Webster, G., and Ladias, J. A. A. (2001) *J. Mol. Biol.* **308,** 963–973
38. Thompson, J. D., Gibson, T. J., Plewniak, F., Jeanmougin, F., and Higgins, D. G. (1997) *Nucleic Acids Res.* **24,** 4876–4882